

DURATION AWARE SCHEDULING FOR ASR SERVING UNDER WORKLOAD DRIFT

Darshan Makwana*
Sprinklr
Gurugram, India

Yash Jogi
Sprinklr
Gurugram, India

Harsh Kotta
Sprinklr
Gurugram, India

Aayush Kubba
Sprinklr
Gurugram, India

ABSTRACT

Scheduling policies in large-scale Automatic Speech Recognition (ASR) serving pipelines play a key role in determining end-to-end (E2E) latency. Yet, widely used serving engines rely on first-come-first-served (FCFS) scheduling, which ignores variability in request duration and leads to head-of-line blocking under workload drift. We show that audio duration is an accurate proxy for job processing time in ASR models such as Whisper, and use this insight to enable duration-aware scheduling. We integrate two classical algorithms, Shortest Job First (SJF) and Highest Response Ratio Next (HRRN), into vLLM and evaluate them under realistic and drifted workloads. On LibriSpeech test-clean, compared to baseline, SJF reduces median E2E latency by up to 73% at high load, but increases 90th-percentile tail latency by up to 97% due to starvation of long requests. HRRN addresses this trade-off: it reduces median E2E latency by up to 28% while bounding tail-latency degradation to at most 24%. These gains persist under workload drift, with no throughput penalty and < 0.1 ms scheduling overhead per request.

1 INTRODUCTION

End-to-end latency is a critical quality-of-service metric for ASR systems. In interactive applications such as voice assistants Li et al. (2017), real-time captioning Xue et al. (2022), and simultaneous interpretation Ma et al. (2020), users expect responses that are nearly instantaneous. Hence, any noticeable delay can reduce usability and overall user satisfaction.

Popular speech-to-text (STT) models, such as Whisper Radford et al. (2023), are often deployed using inference engines like vLLM Kwon et al. (2023) and Orca Yu et al. (2022), which typically use a first-come-first-served (FCFS) scheduling policy. FCFS is simple and does not require any knowledge regarding the workload in advance. However, it can become inefficient under heavy load or when request distributions vary: long-running requests can block shorter ones, increasing queue delays and average latency. Figure 1 illustrates this with a simple example. In the given example, merely reordering requests by estimated job length reduces the average latency by around 1.4 times.

To overcome the limitations of FCFS under variable workloads, scheduling algorithms that account for job processing time can produce more efficient execution orders and in turn reduce queuing delays. In this paper, we analyze and exploit the correlation between audio duration and job processing time to estimate job lengths and apply this estimation to two classical scheduling algorithms. The first is Shortest Job First (SJF) Silberschatz et al. (2018), which prioritizes shorter requests to minimize average waiting time. The second is Highest Response Ratio Next (HRRN) Silberschatz et al. (2018), which incorporates both waiting time and estimated job length to mitigate starvation of longer jobs.

We integrate the two algorithms, SJF and HRRN, into vLLM’s engine and evaluate them on two workloads: the LibriSpeech Panayotov et al. (2015) *test-clean* split and a synthetic workload derived from the LibriSpeech dataset with a uniform duration distribution, in order to study robustness under workload drift.

On the LibriSpeech dataset, we find that SJF, compared to baseline, reduces median end-to-end latency by up to 73% and median time to first token by up to 93% at high workload, with no through-

*Correspondence to: Darshan Makwana (darshan.makwana@sprinklr.com)

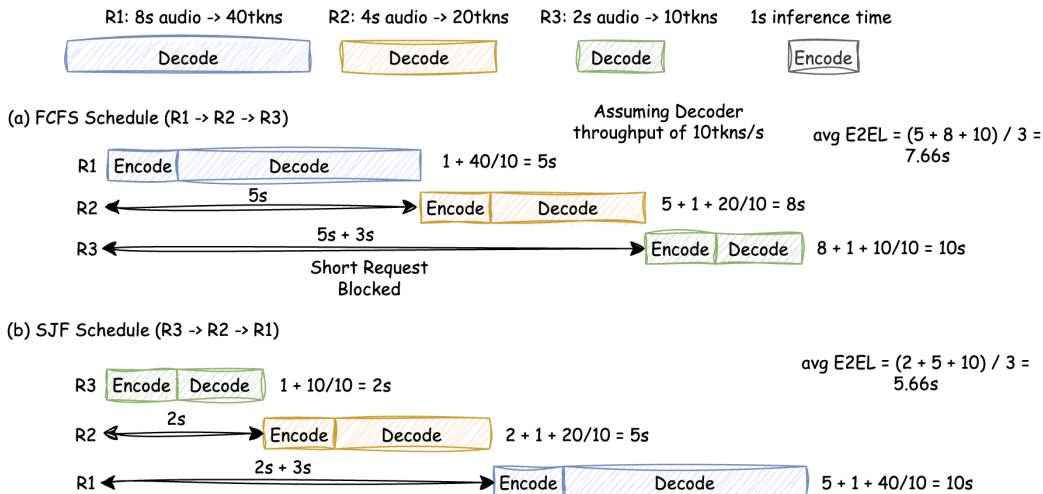


Figure 1: Toy example illustrating head-of-line blocking under FCFS and the benefit of duration-aware scheduling. Three requests arrive in order R_1, R_2, R_3 with audio durations 8 s, 4 s, and 2 s. We assume a constant encoder cost of 1 s per request and a decoding rate of 5 output tokens/s, yielding 40, 20, and 10 output tokens, respectively. Under FCFS, serving R_1 first delays the two shorter requests and yields an average end-to-end latency of $(5+8+10)/3 = 7.66$ s. Reordering by shortest job first (SJF) reduces the average to $(2+5+10)/3 = 5.66$ s (a $1.4\times$ improvement). All numbers are illustrative and not intended to match measured system timings.

put penalty. These gains persist across workloads: even on the synthetic split, SJF achieves up to a 67% reduction in median end-to-end latency, confirming that the improvements arise from queue reordering rather than exploiting natural skew in audio durations present in the LibriSpeech dataset. Moreover, HRRN provides a practical alternative, delivering consistent median improvements while bounding 90th-percentile tail latency degradation to at most 24%, compared to 97% for SJF, compared to baseline. Additionally, both policies incur less than 0.1 ms of scheduling overhead per request. Overall, our findings show that duration-aware policies offer an effective, deployment-ready enhancement for improving ASR responsiveness.

2 RELATED WORK

LLM serving systems. Modern inference engines such as Orca (Yu et al., 2022) and vLLM (Kwon et al., 2023) introduced iteration-level scheduling and paged KV-cache management, forming the backbone of current serving stacks. Sarathi-Serve (Agrawal et al., 2024) eliminates decode stalls via chunked prefill, while DistServe (Zhong et al., 2024) and Splitwise (Patel et al., 2024) disaggregate prefill and decode phases across GPUs. All of these systems default to FCFS scheduling and are therefore susceptible to head-of-line blocking when request durations vary. Moreover, due to the architectural similarities between LLMs and Whisper, these serving frameworks are also commonly used for Whisper.

Scheduling for LLM inference. FastServe (Wu et al., 2023) applies a skip-join multi-level feedback queue (MLFQ) to LLM serving, assigning requests to priority queues based on tokens generated so far. Fu et al. (Fu et al., 2024) train a small ranking model to predict relative output lengths and approximate SJF ordering, achieving up to $2.8\times$ lower latency on chatbot workloads. Andes (Liu et al., 2024) introduces a quality-of-experience metric and schedules at token granularity to maximize user satisfaction. Sheng et al. (Sheng et al., 2024) propose a Virtual Token Counter for fair scheduling that accounts for both input and output tokens. These methods all target text-based LLM workloads where output length is unknown a priori and must be predicted or estimated online.

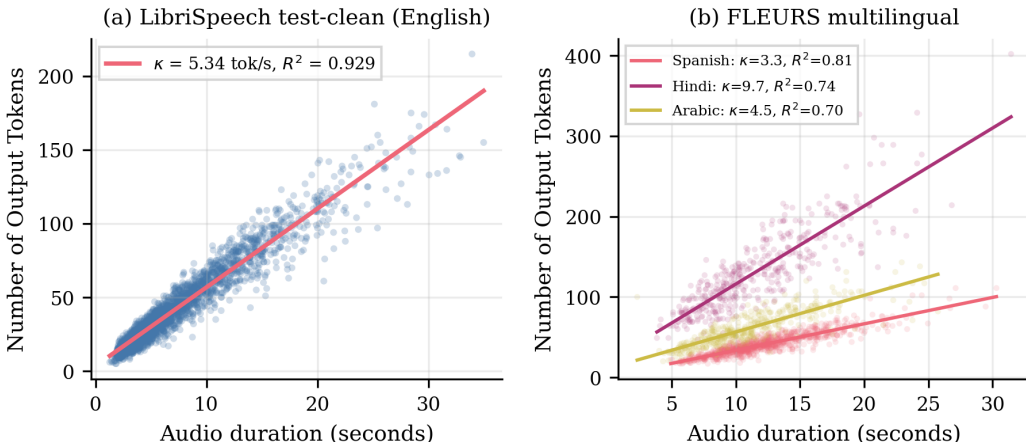


Figure 2: Scatter plots showing the relationship between audio duration and ASR output token count. (a) On the LibriSpeech English test set, token count increases linearly with audio duration, indicating a strong correlation. (b) On the FLEURS test sets for Spanish, Hindi, and Arabic, the linear duration–token relationship is maintained, demonstrating that this correlation generalizes across typologically diverse languages.

Output length prediction. Several works predict LLM output lengths to improve scheduling or memory allocation. S3 (Jin et al., 2023) uses a classification model to predict sequence lengths for KV-cache sizing. Zheng et al. (Zheng et al., 2023) let the LLM itself predict its response length before generation. Magnus (Cheng et al., 2024) combines semantic features with HRRN scheduling. Qiu et al. (Qiu et al., 2024) train a BERT proxy model for speculative SJF. All of these approaches incur non-trivial overhead: either an auxiliary predictor that consumes GPU cycles, or self-prediction tokens that delay the actual response. We draw inspiration from these works and adapt these ideas to the problem of ASR output length prediction.

Size-based scheduling. Prioritizing shorter jobs originates in classical scheduling theory (Silberschatz et al., 2018). Harchol-Balter et al. (Harchol-Balter et al., 2003) show that Shortest Remaining Processing Time (SRPT) scheduling yields large mean response time reductions in web servers when file sizes are known, with limited unfairness under heavy-tailed workloads (Bansal & Harchol-Balter, 2001). Clockwork (Gujarati et al., 2020) exploits deterministic DNN execution times for predictable latency. Our work draws on this tradition: in ASR serving, audio duration plays the role of file size a freely available signal for job length that requires no prediction.

The central difference between our approach and prior scheduling work for LLM inference is the source of the job-length signal. For text-based LLMs, output length is fundamentally unpredictable, forcing systems to train auxiliary models (Fu et al., 2024; Jin et al., 2023; Qiu et al., 2024), prompt the LLM itself (Zheng et al., 2023), or rely on heuristic features (Cheng et al., 2024). In ASR workloads, audio duration is known at request arrival and correlates strongly with processing time (§3), providing a practically zero-overhead scheduling signal that is trivially deployable solution.

3 METHODOLOGY

This section first analyzes the relationship between audio duration and job processing time, followed by description of the two scheduling algorithms considered in our study.

3.1 CORRELATION BETWEEN AUDIO DURATION AND JOB PROCESSING TIME

In encoder–decoder STT models such as Whisper, an input audio is processed by the Whisper encoder in fixed-length segments of 30 seconds, leading to near-constant encoding time per segment. Decoding time, however, grows approximately linearly with the number of generated output tokens.

As a result, overall processing time is dominated by decoding and is largely determined by the number of generated output tokens.

In ASR models, the number of generated output tokens is strongly correlated with the duration of the input audio. This relationship arises from the relatively stable rate of human speech, whereby longer audio segments contain more words and therefore more tokens. We empirically analyze this correlation using the LibriSpeech test-clean set for English and the FLEURS dataset for Spanish, Hindi, and Arabic. Transcriptions are generated using the `whisper-large-v3` ASR model. Figure 2 presents scatter plots of audio duration versus output token count across all the datasets, revealing a clear linear relationship, which can be expressed as:

$$\hat{n} = d \times \kappa \tag{1}$$

where d is audio duration, κ is a language-specific constant, and \hat{n} is the estimated number of output tokens. The values of κ for English, Arabic, and Spanish are reported in Figure 2 along with their estimation errors. Since job processing time is proportional to token count, audio duration provides a reliable estimate of processing time. Because scheduling algorithms depend only on the relative ordering of jobs, exact job time estimates are not required. Therefore, we use audio duration as a proxy for job processing time in the scheduling algorithms described below.

3.2 SCHEDULING POLICIES

Shortest Job First (SJF). SJF prioritizes shorter jobs from the pool of incoming requests, which minimizes the average waiting time across all jobs (Silberschatz et al., 2018). If multiple jobs have the same duration, earlier arrivals are prioritized. We implement SJF using a min-heap, which has $O(\log n)$ cost for both insertion and deletion.

Although SJF does reduce average waiting time, it can cause starvation for long jobs when short jobs continuously arrive, as long requests may be delayed indefinitely (Silberschatz et al., 2018; Bansal & Harchol-Balter, 2001).

Highest Response Ratio Next (HRRN). To address the starvation issue inherent in SJF, HRRN incorporates both waiting time and estimated job duration when making scheduling decisions. Jobs are ordered according to their response ratio, defined as:

$$\text{Response Ratio} = \frac{\text{Waiting Time} + \text{Estimated Job Time}}{\text{Estimated Job Time}}.$$

The estimated job time in the above equation is derived from the audio duration using the linear relationship in Equation 1. Because HRRN only requires relative ordering, the exact token count need not be precise, audio duration d can be used directly as the estimated job time. Jobs with higher response ratios are scheduled first, allowing requests that have waited longer to gradually gain priority while still favoring shorter jobs (Silberschatz et al., 2018).

4 EXPERIMENTS

4.1 SETUP

For all experiments, we use the Whisper model as the ASR model, specifically the `whisper-large-v3` variant with $1.5B$ parameters. The model is served using vLLM with the `openai-audio` backend, with maximum output length of 448 tokens, and chunked pre-fill (Agrawal et al., 2024) enabled. We configure vLLM with a maximum batch size of 256 (the default setting) and a GPU memory utilization target of 95%. All experiments are conducted on a single NVIDIA A100 GPU with 40 GB HBM2e memory, running on CUDA 12.1. To study how scheduling policies perform under workloads with different characteristics, we use two datasets derived from the LibriSpeech test-clean subset:

Original LibriSpeech split. This is Librispeech as it is with audio durations ranging from 1 to 35 s with $\mu=7.4$ s and $\sigma=5.15$ s. The distribution is right-skewed, with the majority of utterances being short, reflecting realistic ASR serving conditions. Since the dataset has a right-skewed duration

Table 1: LibriSpeech test-clean: Latency comparison across request rates (ms). Parenthesized values show relative change versus FCFS. Bold values indicate the highest value among the three policies. Green : >3% improvement; red : >3% degradation.

Rate	P50 TTFT (ms) ↓			P50 E2EL (ms) ↓			P90 E2EL (ms) ↓		
	FCFS	SJF	HRRN	FCFS	SJF	HRRN	FCFS	SJF	HRRN
1	64.6	61.5 (-5%)	73.3 (+13%)	88.2	84.9 (-4%)	96.4 (+9%)	143.8	141.6 (-2%)	155.7 (+8%)
5	64.7	62.8 (-3%)	64.4	112.4	108.9 (-3%)	112.5	276.7	261.3 (-6%)	275.9
10	118.6	115.5 (-3%)	115.1 (-3%)	213.0	200.8 (-6%)	195.6 (-8%)	742.7	682.5 (-8%)	681.7 (-8%)
15	192.0	144.2 (-25%)	198.3 (+3%)	547.9	518.3 (-5%)	598.3 (+9%)	1561.6	1467.9 (-6%)	1615.4 (+3%)
20	1467.8	193.3 (-87%)	1173.9 (-20%)	2728.7	1325.8 (-51%)	2231.2 (-18%)	3954.8	7094.6 (+79%)	4996.6 (+26%)
25	4273.4	296.3 (-93%)	2867.3 (-33%)	5423.8	1486.8 (-73%)	3897.9 (-28%)	8334.4	16405.3 (+97%)	10347.3 (+24%)

distribution, where the majority of utterances are short, precisely the regime where SJF thrives, because the queue is dominated by quick jobs that SJF can rapidly drain. A natural concern is whether the observed gains are an artifact of this skew: perhaps SJF only helps when most requests are already short and a few long outliers cause head-of-line blocking.

Synthetic LibriSpeech Split. To disentangle the effect of duration *ordering* from the effect of duration *distribution shape*, we construct a *synthetic split* from six LibriSpeech with the exact target durations {5, 10, 15, 20, 25, 30} s. This produces a discrete-uniform distribution with higher mean ($\mu=17.5$ s) and higher variance ($\sigma\approx 8.5$ s) than LibriSpeech. Crucially, this removes the right-skew: short and long jobs are now equally likely, and the mean job is substantially longer. If scheduling gains collapse under this flat, heavy workload, we would conclude the benefit was distribution-dependent. If the gains persist, this indicates that priority reordering is valuable and that the improvements observed on LibriSpeech are not solely attributable to its right-skewed duration distribution.

We simulate a realistic serving scenario in which audio requests arrive as a continuous stream following a Poisson process with a burstiness factor of 1.0. To evaluate performance under varying workload intensities, we vary the request arrival rate from 1 to 25 requests per second. For each configuration, the simulation is run for 5 minutes. To ensure a fair comparison, all scheduling policies are evaluated using identical arrival sequences.

Evaluation Metrics. We evaluate the policies using metrics that reflect system performance and user experience. End-to-end latency (E2EL) measures the total time from request arrival to transcription completion, including queuing, prefill, and decode phases. Time to first token (TTFT) captures the delay until the first output appears, reflecting perceived responsiveness. We report the 50th percentile (*P50*) and 90th percentile (*P90*) for each metric. *P50* captures the typical user experience, which is the latency at or below which half of all requests complete, while *P90* reveals tail behavior, quantifying how the slowest requests are affected by the scheduling policy. Reporting both is critical for evaluating scheduling trade-offs: a policy that dramatically improves *P50* may do so at the expense of *P90*, trading better median experience for degraded worst-case reliability.

4.2 RESULTS

Figure 3 and 4 show the performance of the three scheduling policies on the original LibriSpeech split. To examine the performance under different workload conditions, we divide the workload into three request-rate ranges: low (1–10 req/s), moderate (10–20 req/s), and heavy (20–25 req/s). The paragraphs below summarize each policy’s performance in these ranges; a table of the numerical results appears in Table 1. All percentage comparisons done below are made relative to FCFS.

Under low load, resources are sufficient to handle incoming requests and queues rarely form, so all policies perform similarly. However, at the upper end of this range at 10 req/s, both SJF and HRRN show measurable improvements: SJF reduces *P50* and *P90* E2EL by 6% and 8%, respectively, while HRRN achieves reductions of 8% for both metrics. This indicates that even when the system is lightly loaded, reordering requests according to estimated job size can yield latency benefits.

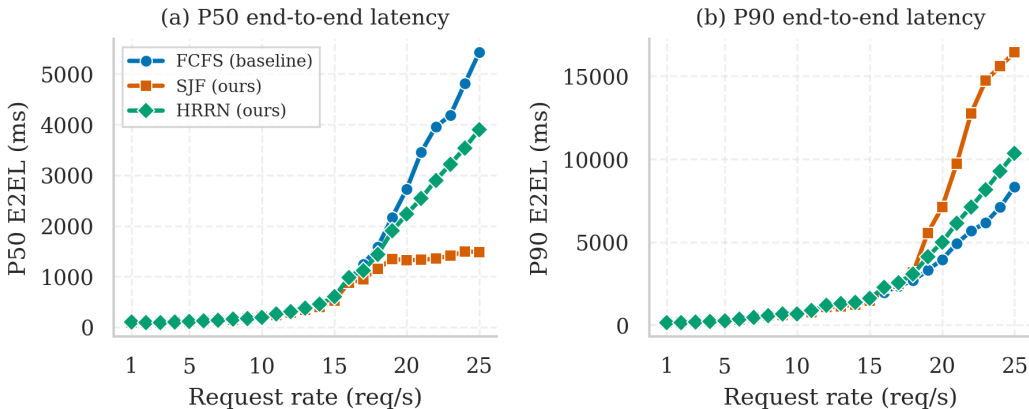


Figure 3: LibriSpeech test-clean: End-to-end latency scaling (1–25 req/s). (a) SJF reduces $P50$ E2EL by up to 73% at 25 req/s, (b) while $P90$ E2EL reveals the starvation trade-off at high load.

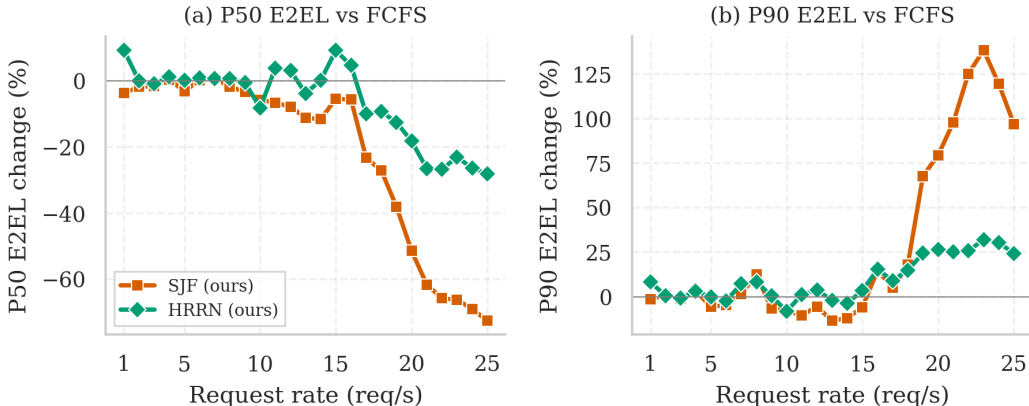


Figure 4: LibriSpeech test-clean: Percentage change in E2EL versus FCFS (1–25 req/s). Negative values indicate improvement. SJF’s $P50$ gains deepen monotonically with load, while $P90$ degradation emerges beyond 15 req/s.

As the request rate enters the moderate range and approaches the system’s service capacity, queues begin to lengthen, making SJF’s advantages more pronounced. At 17 req/s, SJF reduces $P50$ E2EL by 23%, though $P90$ E2EL begins to show the starvation trade-off with a modest 5% increase. HRRN lowers $P50$ E2EL by 10% while its $P90$ E2EL increases by 9%. HRRN’s weaker $P50$ improvement relative to SJF reflects its aging mechanism: by gradually promoting long-waiting jobs, it sacrifices some median-latency gain to prevent starvation a trade-off that becomes more consequential as queue depth grows. The moderate-load regime thus represents a practical sweet spot for SJF: the system is sufficiently busy to exploit job reordering, yet not saturated enough to cause severe starvation for longer jobs.

Under heavy load, SJF’s improvements become even more pronounced. At 23 req/s, SJF reduces $P50$ E2EL by 66%. However, this comes at a significant cost for tail latency, as $P90$ E2EL increases by 138%. In this case, HRRN provides a practical middle ground: it reduces $P50$ E2EL only by 23% while limiting $P90$ E2EL degradation to 32%. Moreover, results for TTFT, a metric more directly reflective of queuing delay, which show even greater improvements, are provided in Appendix A.1.

Figure 5 and 6 present the same evaluation on the synthetic split. Table 2 reports the corresponding numerical results. The two main findings are:

SJF E2EL gains persist. At 25 req/s, SJF reduces $P50$ E2EL by 67%. At 20 req/s, SJF delivers 65% $P50$ E2EL reduction, showing that end-to-end latency benefits generalizes across this workload

Table 2: Synthetic split: Latency comparison across request rates (ms). Parenthesized values show relative change versus FCFS. Bold values indicate the highest value among the three policies. Green : $> 3\%$ improvement; red : $> 3\%$ degradation.

Rate	P50 TTFT (ms) ↓			P50 E2EL (ms) ↓			P90 E2EL (ms) ↓		
	FCFS	SJF	HRRN	FCFS	SJF	HRRN	FCFS	SJF	HRRN
1	64.0	67.1 (+5%)	68.6 (+7%)	84.8	88.3 (+4%)	89.9 (+6%)	158.0	162.8 (+3%)	164.0 (+4%)
5	66.0	68.4 (+4%)	68.8 (+4%)	117.7	121.1 (+3%)	122.1 (+4%)	242.2	262.9 (+9%)	260.3 (+7%)
10	120.3	126.8 (+5%)	124.3 (+3%)	214.8	229.3 (+7%)	239.5 (+11%)	741.1	849.0 (+15%)	881.6 (+19%)
15	2654.0	267.1 (−90%)	2263.5 (−15%)	4788.6	2287.3 (−52%)	4520.1 (−6%)	7529.9	8902.4 (+18%)	9635.5 (+28%)
20	6661.2	906.7 (−86%)	4702.7 (−29%)	8686.9	3079.7 (−65%)	6939.6 (−20%)	14325.2	22478.8 (+57%)	16664.3 (+16%)
25	9923.9	1574.4 (−84%)	6577.1 (−34%)	12123.3	3966.3 (−67%)	9340.9 (−23%)	19664.3	25336.7 (+29%)	22378.3 (+14%)

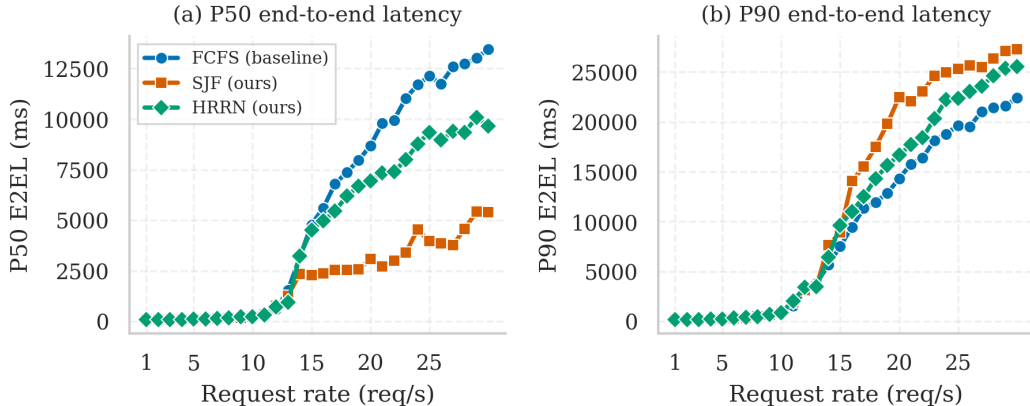


Figure 5: Synthetic split: End-to-end latency scaling (1–30 req/s). (a) SJF’s $P50$ E2EL advantage (−67% at 25 req/s) persists under a uniform duration distribution, (b) while $P90$ E2EL degradation is moderated compared to LibriSpeech’s right-skewed workload.

distribution as well, which has a more uniform duration distribution than the LibriSpeech test-clean dataset.

Tail penalty is moderated. Despite the wider duration range, SJF’s tail cost is lower than on LibriSpeech: at 25 req/s, $P90$ E2EL inflation is 29% versus 97%; at 20 req/s, 57% versus 79%. HRRN’s tail penalty also shrinks (14% versus 24% at 25 req/s). The explanation is distributional: LibriSpeech’s right-skew means the queue is flooded with short requests that SJF continuously prioritizes, starving the few long outliers indefinitely. Under a uniform distribution, long requests arrive at the same frequency as short ones, so the queue is less persistently dominated by short jobs and starvation episodes are shorter-lived.

Another important consideration is whether scheduling improvements affect overall throughput of the system. Figure 7 presents the request rate versus throughput for all three policies. All of them achieve identical request throughput on both datasets. There is no measurable difference because the only overhead is the scheduling decision, which adds on average < 0.1 ms per request, which is negligible compared to the $\sim 60 - 100$ ms processing time for one decoder step in ASR.

5 LIMITATIONS AND FUTURE WORK

Silence sensitivity. Our duration-based estimator assumes that spoken content fills most of the audio clip. However, when recordings contain extended silence segments (e.g., pauses, leading/trailing silence), the estimator can overestimate the number of output tokens, since silent regions produce no transcription tokens. A natural mitigation is to apply a voice activity detection (VAD) module as a preprocessing step, computing d as the sum of speech-active segments rather than the raw file duration. Lightweight VAD models (e.g., Silero VAD (Silero Team, 2024)) add < 5 ms per utterance and could be integrated at the API endpoint with negligible overhead.

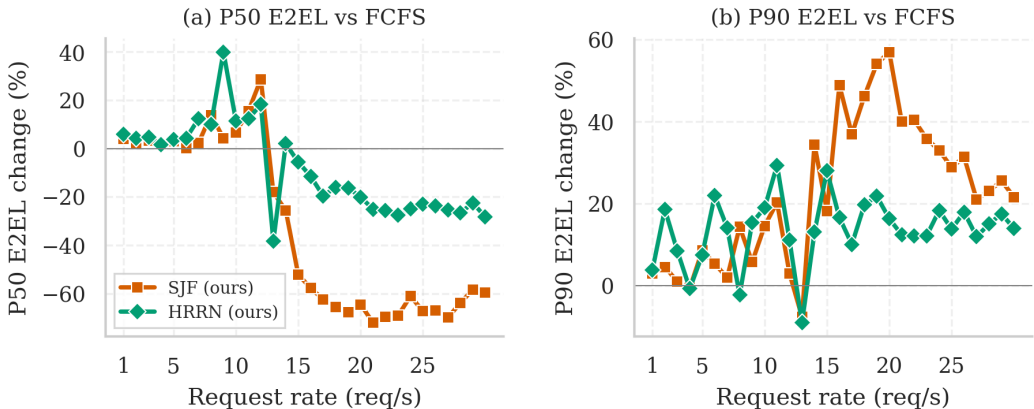


Figure 6: Synthetic split: Percentage change in E2EL versus FCFS (1–30 req/s). SJF’s E2EL gains match LibriSpeech, confirming reordering benefits are not an artifact of the natural duration skew.

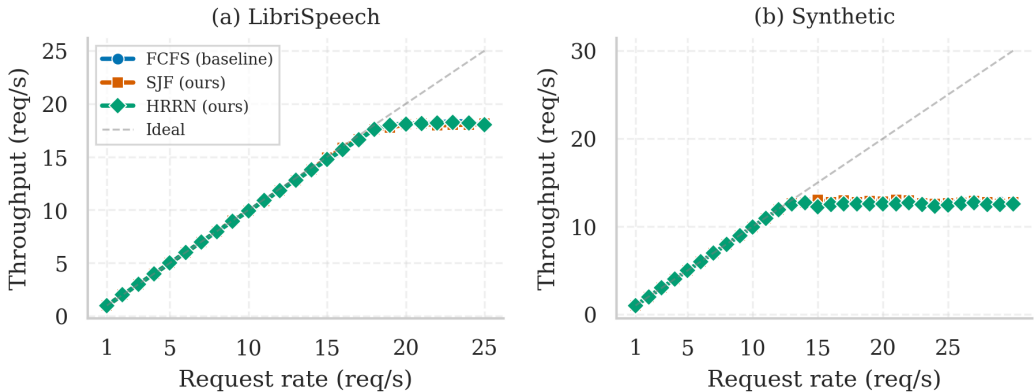


Figure 7: Request throughput for both workloads. All scheduling policies achieve identical throughput, saturating at ~ 18 req/s on LibriSpeech and ~ 13 req/s on the synthetic split, confirming negligible scheduling overhead.

Adaptive κ . The current system employs a fixed κ across all requests. In multilingual deployments, where languages exhibit different tokenization densities, as shown in Figure 2, this assumption may be limiting and can lead to suboptimal estimation accuracy.

Dynamic policy switching. Our experiments evaluate each scheduling policy in isolation. A production system could monitor queue depth, tail-latency percentiles, and starvation indicators in real time, dynamically switching between FCFS, SJF, and HRRN to match the current load regime.

6 CONCLUSION

We show that first-come-first-served scheduling has clear limitations for ASR serving when request durations vary, and that audio duration is a reliable, zero-overhead proxy for job length in encoder-decoder models such as Whisper. After integrating SJF and HRRN into vLLM, we observe up to 73% lower median E2E latency and up to 93% lower median TTFT on LibriSpeech at high load. These improvements persist under workload drift, while HRRN bounds tail-latency degradation to at most 24%. Duration-aware scheduling is a simple, deployment-ready lever for improving user-perceived latency in production ASR systems.

REFERENCES

- Amey Agrawal, Nitin Kedia, Ashish Panwar, Jayashree Mohan, Nipun Kwatra, Bhargav S Gulavani, Alexey Tumanov, and Ramachandran Ramjee. Taming throughput-latency tradeoff in LLM inference with Sarathi-Serve. In *USENIX Symposium on Operating Systems Design and Implementation*, 2024.
- Nikhil Bansal and Mor Harchol-Balter. Analysis of SRPT scheduling: Investigating unfairness. In *ACM SIGMETRICS Performance Evaluation Review*, volume 29, pp. 279–290, 2001.
- Ke Cheng, Wen Hu, Zhi Wang, Peng Du, Jianguo Li, and Sheng Zhang. Enabling efficient batch serving for LMaaS via generation length prediction. *arXiv preprint arXiv:2406.04785*, 2024.
- Yichao Fu, Siqi Zhu, Runlong Su, Aurick Qiao, Ion Stoica, and Hao Zhang. Efficient LLM scheduling by learning to rank. In *Advances in Neural Information Processing Systems*, 2024.
- Arpan Gujarati, Reza Karber, Safya Avalos, Prateek Banchhor, Mor Harchol-Balter, and Michael Kozuch. Serving DNNs like clockwork: Performance predictability from the bottom up. In *USENIX Symposium on Operating Systems Design and Implementation*, pp. 443–462, 2020.
- Mor Harchol-Balter, Bianca Schroeder, Nikhil Bansal, and Mukesh Agrawal. Size-based scheduling to improve web performance. *ACM Transactions on Computer Systems*, 21:207–233, 2003.
- Yunho Jin, Chun-Feng Wu, David Brooks, and Gu-Yeon Wei. s^3 : Increasing GPU utilization during generative inference for higher throughput. In *Advances in Neural Information Processing Systems*, volume 36, 2023.
- Woosuk Kwon, Zhuohan Li, Siyuan Zhuang, Ying Sheng, Lianmin Zheng, Cody Hao Yu, Joseph E Gonzalez, Hao Zhang, and Ion Stoica. Efficient memory management for large language model serving with PagedAttention. In *Proceedings of the 29th Symposium on Operating Systems Principles*, pp. 611–626, 2023.
- Bo Li, Tara N Sainath, Arun Narayanan, Joe Caroselli, Michiel Bacchiani, Ananya Misra, Izhak Shafran, Hagen Soltau, Rohit Prabhavalkar, et al. Acoustic modeling for Google Home. In *Interspeech*, pp. 399–403, 2017.
- Jiachen Liu, Zhiyu Wu, Jae-Won Chung, Fan Lai, Myungjin Lee, and Mosharaf Chowdhury. Andes: Defining and enhancing quality-of-experience in LLM-based text streaming services. *arXiv preprint arXiv:2404.16283*, 2024.
- Xutai Ma, Juan Pino, and Philipp Koehn. SimulMT to SimulST: Adapting simultaneous text translation to end-to-end simultaneous speech translation. In *Asia-Pacific Chapter of the Association for Computational Linguistics*, pp. 582–587, 2020.
- Vassil Panayotov, Guoguo Chen, Daniel Povey, and Sanjeev Khudanpur. LibriSpeech: an ASR corpus based on public domain audio books. In *IEEE International Conference on Acoustics, Speech and Signal Processing*, pp. 5206–5210, 2015.
- Pratyush Patel, Esha Choukse, Chaojie Zhang, Aashaka Shah, Íñigo Goiri, Saeed Maleki, and Riccardo Bianchini. Splitwise: Efficient generative LLM inference using phase splitting. In *International Symposium on Computer Architecture*, 2024.
- Haoran Qiu, Weichao Mao, Archit Patke, Shengkun Cui, Saurabh Jha, Chen Wang, Hubertus Franke, Zbigniew T Kalbarczyk, Tamer Başar, and Ravishankar K Iyer. Efficient interactive LLM serving with proxy model-based sequence length prediction. *arXiv preprint arXiv:2404.08509*, 2024.
- Alec Radford, Jong Wook Kim, Tao Xu, Greg Brockman, Christine McLeavey, and Ilya Sutskever. Robust speech recognition via large-scale weak supervision. In *International Conference on Machine Learning*, pp. 28492–28518. PMLR, 2023.
- Ying Sheng, Shiyi Cao, Dacheng Li, Banghua Zhu, Zhuohan Li, Danyang Zhuo, Joseph E Gonzalez, and Ion Stoica. Fairness in serving large language models. In *USENIX Symposium on Operating Systems Design and Implementation*, 2024.

Abraham Silberschatz, Peter B Galvin, and Greg Gagne. *Operating System Concepts*. Wiley, 10th edition, 2018.

Silero Team. Silero VAD: pre-trained enterprise-grade voice activity detector. <https://github.com/snakers4/silero-vad>, 2024.

Yuxin Wang, Yuhan Chen, Zeyu Li, Zhenheng Tang, Rui Guo, Xin Wang, Qiang Wang, Amelie Chi Zhou, and Xiaowen Chu. Towards efficient and reliable LLM serving: A real-world workload study. *arXiv preprint arXiv:2401.17644*, 2024.

Bingyang Wu, Yinmin Zhong, Zili Zhang, Gang Huang, Xuanzhe Liu, and Xin Jin. Fast distributed inference serving for large language models. *arXiv preprint arXiv:2305.05920*, 2023.

Hongwei Xue, Tiankai Hang, Yanhong Zeng, Yuchong Sun, Bei Liu, Huan Yang, Jianlong Fu, and Baining Guo. Advancing high-resolution video-language representation with large-scale video transcriptions. In *IEEE/CVF Conference on Computer Vision and Pattern Recognition*, 2022.

Gyeong-In Yu, Joo Seong Jeong, Geon-Woo Kim, Soojeong Kim, and Byung-Gon Chun. Orca: A distributed serving system for transformer-based generative models. In *USENIX Symposium on Operating Systems Design and Implementation*, pp. 521–538, 2022.

Zangwei Zheng, Xiaozhe Ren, Fuzhao Xue, Yang Luo, Xin Jiang, and Yang You. Response length perception and sequence scheduling: An LLM-empowered LLM inference pipeline. In *Advances in Neural Information Processing Systems*, volume 36, pp. 65517–65530, 2023.

Yinmin Zhong, Shengyu Liu, Junda Chen, Jianbo Hu, Yibo Zhu, Xuanzhe Liu, Xin Jin, and Hao Zhang. DistServe: Disaggregating prefill and decoding for goodput-optimized large language model serving. In *USENIX Symposium on Operating Systems Design and Implementation*, 2024.

A APPENDIX

A.1 TIME TO FIRST TOKEN ANALYSIS

While the main text focuses on end-to-end latency (E2EL), time to first token (TTFT) provides complementary insight into queuing behavior. Because TTFT measures only the delay before decoding begins, it isolates the scheduling decision’s direct impact on queue wait time.

Figure 8 shows TTFT scaling on LibriSpeech. At heavy load (20–25 req/s), SJF reduces $P50$ TTFT by up to 93% from 4273 ms under FCFS to 296 ms, demonstrating that priority scheduling effectively reduces queuing delay for the majority of requests. Even at the $P90$ percentile, SJF maintains sub-second TTFT up to 15 req/s. HRRN achieves -33% $P50$ TTFT at 25 req/s while limiting $P90$ TTFT degradation relative to SJF. The corresponding percentage changes are shown in Figure 9.

Figure 10 shows TTFT on the synthetic split. SJF achieves an 84% $P50$ TTFT reduction at 25 req/s, confirming that TTFT improvements are driven by queue reordering rather than by exploiting large duration gaps. Percentage changes are shown in Figure 11.

A.2 BURST WORKLOAD ANALYSIS

The experiments in the main text simulate realistic Poisson arrivals at varying rates. To stress-test scheduling policies under an extreme workload drift scenario, we evaluate a *burst workload* where all 500 requests arrive simultaneously (request rate = ∞). This models sudden traffic spikes common in production (Wang et al., 2024) and represents the worst-case queuing scenario: the scheduler must immediately triage a deep queue with no inter-arrival gaps.

Setup. We run the same whisper-large-v3 model on identical hardware (A100 40 GB). Each policy processes the full LibriSpeech test-clean split (500 utterances) submitted as a single burst. Results are shown in Figure 12.

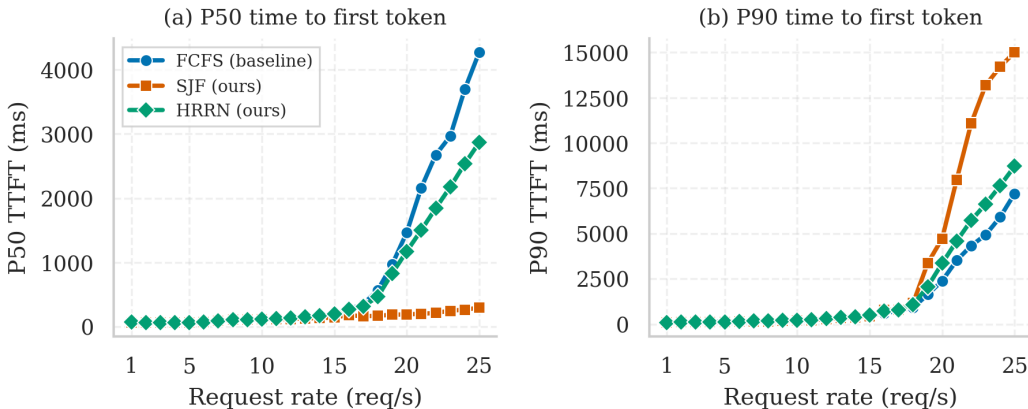


Figure 8: LibriSpeech TTFT scaling (1–25 req/s). SJF keeps P_{50} TTFT below 300 ms at all rates while FCFS exceeds 4 s.

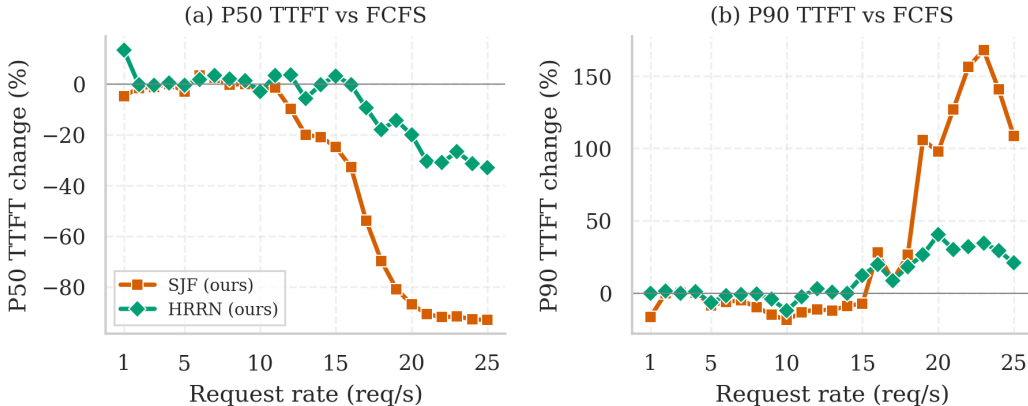


Figure 9: LibriSpeech: percentage change in TTFT versus FCFS (1–25 req/s). SJF’s P_{50} TTFT gains deepen monotonically, reaching -93% at 25 req/s.

Results. Under burst arrival, the differences between policies are smaller than under sustained overload, which is expected since all 500 requests are queued before any completes. SJF reduces P_{50} TTFT by -2.1% and P_{50} E2EL by -3.7% relative to FCFS, while HRRN achieves -9.6% P_{50} TTFT and -10.7% P_{50} E2EL. The moderate gains reflect the fact that with a single burst, the queue drains monotonically—there are no new arrivals to continually refresh the short-job advantage that SJF exploits under sustained load.

Time per output token (TPOT) and inter-token latency (ITL) remain largely unaffected ($< 8\%$ variation), confirming that scheduling overhead does not impair per-token decoding throughput even under maximum queue depth (500 concurrent requests). HRRN’s consistent edge over both FCFS and SJF across all metrics in this setting stems from its ability to balance job priority with accumulated wait time: as the burst progresses, long-waiting requests naturally gain higher response ratios, preventing the extreme starvation that degrades SJF’s tail under sustained overload.

Significance. The burst experiment establishes two practical findings: (1) scheduling benefits persist even under instantaneous load spikes, albeit with smaller magnitude than sustained overload; and (2) HRRN emerges as the preferred policy for unpredictable traffic patterns since it provides consistent improvements without the starvation risk of SJF.

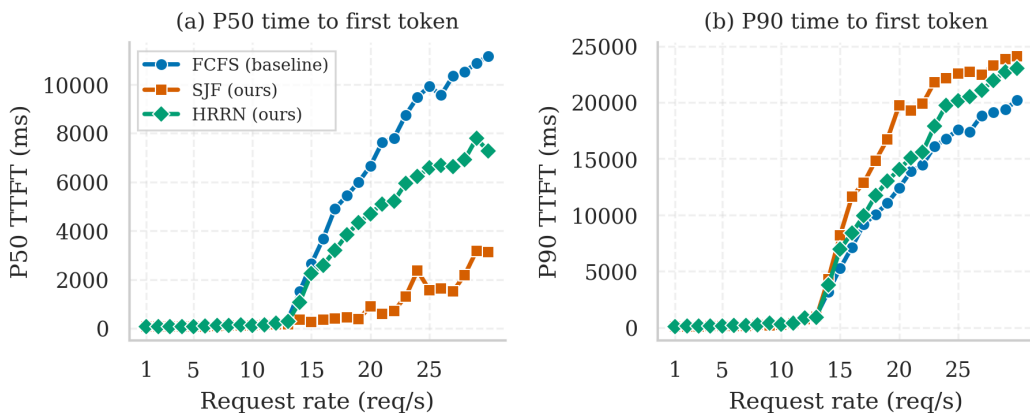


Figure 10: Synthetic split TTFT scaling (1-30 req/s). SJF achieves -84% $P50$ TTFT at 25 req/s, confirming that reordering benefits are independent of duration variance.

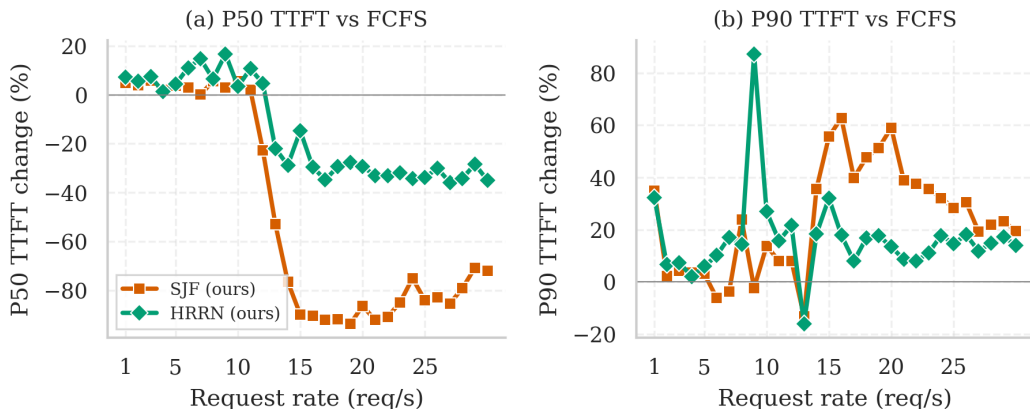


Figure 11: Synthetic split: percentage change in TTFT versus FCFS (1-30 req/s). The pattern closely mirrors LibriSpeech, confirming robustness to duration distribution.

A.3 WHISPER-MEDIUM MODEL SCALING

To assess whether our scheduling findings generalize beyond Whisper-Large-v3 (1.5 B parameters), we repeat the full LibriSpeech evaluation using Whisper-Medium (769 M parameters), roughly half the model size. All other experimental conditions remain identical: the same A100 GPU, identical LibriSpeech test-clean inputs, Poisson arrivals with burstiness 1.0, and 500 completed requests per rate.

Figure 13 presents $P25$ and $P90$ end-to-end latency for request rates 15–25 req/s, the regime where scheduling effects are most pronounced. Two observations stand out:

Higher saturation point. Whisper-Medium saturates at a higher throughput (~ 21 req/s versus ~ 18 req/s for Large-v3), which is expected given the smaller model footprint. This shifts the onset of congestion rightward, meaning that scheduling interventions become critical at higher absolute rates.

Consistent policy ordering. Across 15–25 req/s, the relative ranking of policies mirrors Large-v3: SJF delivers the lowest $P25$ E2EL, reflecting its advantage for the majority of (shorter) requests, while HRRN occupies the middle ground. At the $P90$ tail, the familiar starvation trade-off re-emerges at high load, confirming that the median-vs-tail tension is a structural property of priority scheduling rather than a model-specific artifact.

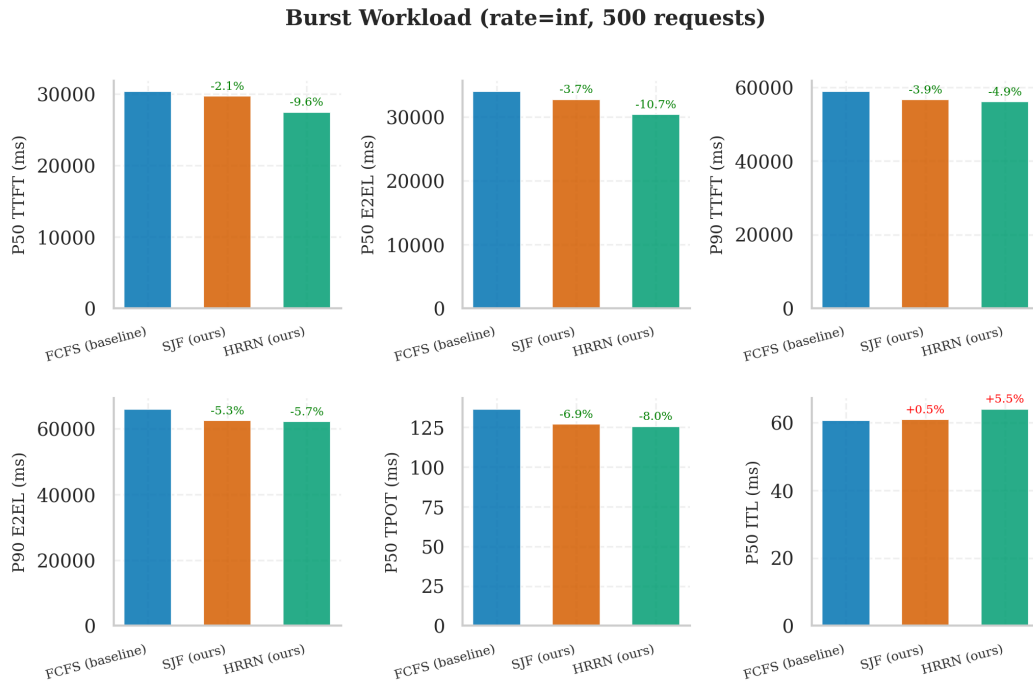


Figure 12: Burst workload results (rate= ∞ , 500 simultaneous requests). Bar heights show absolute metric values; annotations indicate percentage change versus FCFS. HRRN provides the most consistent improvements across all latency metrics.

These results are encouraging: the scheduling policies proposed in this work transfer directly to a smaller model without any re-tuning, and the qualitative behavior large P50 gains with a bounded tail cost controlled by HRRN holds across model scales.

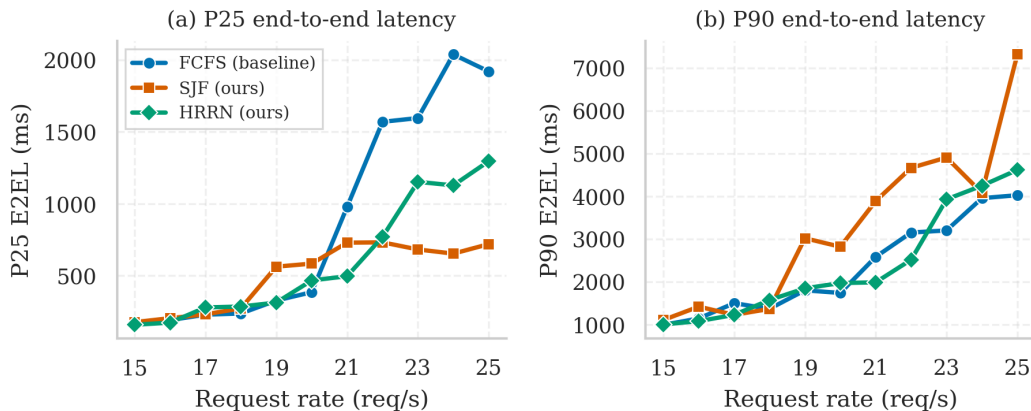


Figure 13: Whisper-Medium E2EL scaling (15–25 req/s). P25 latency (a) shows that SJF benefits the bottom quartile of requests across all rates, while P90 latency (b) reveals the tail cost at high load, consistent with Large-v3 findings.

A.4 IMPLEMENTATION DETAILS

We integrate SJF and HRRN scheduling into vLLM’s v1 engine by modifying five files, totaling \sim 250 lines of new code. The changes require no modification to the core request serialization format (`EngineCoreRequest`).

Output token estimation At the OpenAI-compatible `/v1/audio/transcriptions` endpoint, we capture the raw waveform duration d_i before mel spectrogram extraction:

Listing 1: Duration-based token estimation at the API endpoint.

```
1 duration_s = len(audio_data) / sample_rate
2 estimated_output = max(1, int(duration_s * kappa))
3 sampling_params.extra_args["estimated_output_tokens"] = estimated_output
```

The estimate propagates through `SamplingParams.extra_args` to the scheduler without modifying any serialization format.

Request class. The `Request` class reads `estimated_output_tokens` from `extra_args` at construction, falling back to `max_tokens`:

Listing 2: Request class integration (`v1/request.py`).

```
1 self.estimated_output_tokens = self.max_tokens
2 if (sampling_params.extra_args is not None
3     and "estimated_output_tokens" in sampling_params.extra_args):
4     self.estimated_output_tokens = int(
5         sampling_params.extra_args["estimated_output_tokens"])
```

Queue implementations. `SJFRequestQueue` uses a min-heap keyed by `(estimated_output_tokens, arrival_time, request_id)`, achieving $O(\log n)$ insert/pop. `HRRNRequestQueue` computes response ratios dynamically at each pop in $O(n)$:

Listing 3: SJF and HRRN queue core logic (`request_queue.py`).

```
1 class SJFRequestQueue:
2     def _get_priority(self, req):
3         return (req.estimated_output_tokens, req.arrival_time, req.request_id)
4
5 class HRRNRequestQueue:
6     def _response_ratio(self, req, now):
7         wait = now - req.arrival_time
8         return (wait + req.estimated_output_tokens) / req.estimated_output_tokens
```

Preemption logic. Under memory pressure, SJF evicts the running request with the *largest* \hat{n}_i (longest job first), while HRRN evicts the request with the *lowest* current R_i (least urgent), keeping preemption consistent with each scheduling objective.

Configuration. The scheduling policy is selected via a single CLI flag: `--scheduling-policy sjf` or `--scheduling-policy hrrn`. No other configuration changes are required. The full patch is available in the supplementary material.